

# A common variant in the 3'UTR of the *GRIK4* glutamate receptor gene affects transcript abundance and protects against bipolar disorder

B. S. Pickard<sup>\*†</sup>, H. M. Knight<sup>\*\*</sup>, R. S. Hamilton<sup>§</sup>, D. C. Soares<sup>\*</sup>, R. Walker<sup>¶</sup>, J. K. F. Boyd<sup>\*</sup>, J. Machell<sup>\*</sup>, A. Maclean<sup>\*</sup>, K. A. McGhee<sup>\*</sup>, A. Condie<sup>\*</sup>, D. J. Porteous<sup>\*</sup>, D. St. Clair<sup>||</sup>, I. Davis<sup>§</sup>, D. H. R. Blackwood<sup>‡</sup>, and W. J. Muir<sup>‡</sup>

<sup>\*</sup>Medical Genetics, School of Clinical and Molecular Medicine, Molecular Medicine Centre, University of Edinburgh, Edinburgh EH4 2XU, United Kingdom;

<sup>§</sup>Department of Biochemistry, University of Oxford, Oxford OX1 3QU, United Kingdom; <sup>¶</sup>Neuropathology Unit, Wilkie Building, University of Edinburgh, Edinburgh EH8 9AG, United Kingdom; <sup>||</sup>Institute of Medical Sciences, University of Aberdeen, Aberdeen AB25 2ZD, United Kingdom; and <sup>‡</sup>Division of Psychiatry, University of Edinburgh, Royal Edinburgh Hospital, Edinburgh EH10 5HF, United Kingdom

Edited by Edward G. Jones, University of California, Davis, CA, and approved August 19, 2008 (received for review January 23, 2008)

**Underactivity of the glutamatergic system is an attractive model for the pathophysiology of several major mental illnesses. We previously described a chromosome abnormality disrupting the kainate class ionotropic glutamate receptor gene, *GRIK4/KA1*, in an individual with schizophrenia and learning disability (mental retardation). We also demonstrated in a case-control study that two physically separated haplotypes within this gene were significantly associated with increased risk of schizophrenia and decreased risk of bipolar disorder, respectively. The latter protective haplotype was located at the 3' end of the gene. We now report the identification from carriers of the protective haplotype of a deletion variant within the 3' untranslated region of the gene. The deletion allele also was found to be negatively associated with bipolar disorder in both initial ( $P = 0.0000019$ ) and replication ( $P = 0.0107$ ) case-control studies. Expression studies indicated that deletion-carrying mRNA transcripts were relatively more abundant. We postulate that this may be a direct consequence of the differences in the RNA secondary structures predicted for the insertion and deletion alleles. These data suggest a mechanism whereby the genetic protective effect is mediated through increased kainate receptor expression.**

case-control association | indel | RNA structure | hippocampus | mental illness

The involvement of aberrant glutamatergic neurotransmission in psychiatric illnesses, particularly schizophrenia, has been proposed on the basis of the behavioral effects of glutamate antagonists and altered expression levels of receptors in postmortem brain tissue from affected persons (1–7). We previously described a complex chromosomal rearrangement involving inversion and translocation events in an individual diagnosed with schizophrenia and learning disability (*Diagnostic and Statistical Manual of Mental Disorders IV* classification: mental retardation). One of the break-points on chromosome 11 disrupted the *GRIK4* gene encoding a high-affinity kainate-type ionotropic glutamate receptor subunit, KA1 (8). This gene is expressed in the cerebral cortex and in the dentate gyrus of the hippocampus (9–14). Kainate receptor expression also has been directly implicated in the pathophysiology of schizophrenia (15–18). In a tagging single-nucleotide polymorphism (SNP) case-control association study, we previously identified two physically separated haplotypes within *GRIK4* that affected the risk of severe mental illness in the wider Scottish population (8). The first of these, a 3-SNP haplotype located between exons 3 and 7, predisposes carrier individuals to schizophrenia ( $P = 0.0005$ ; odds ratio [OR] = 1.453; 95% confidence interval [CI] = 1.182–1.787). The second, a 2-SNP haplotype (GC; SNPs rs2282586 and rs1944522), demonstrated a greater statistical significance ( $P = 0.0002$ ; OR = 0.624; 95% CI = 0.485–0.802) and exhibited a protective effect against bipolar disorder for carrier individuals. Both haplotypes survived correction for multiple testing. The

associated SNPs identified in the latter haplotype are located  $\approx 300$  bp upstream and  $\approx 5800$  bp downstream, respectively, of the predicted *GRIK4* gene's mRNA polyadenylation signal.

In this paper, we describe the identification of an insertion/deletion (indel) variant in the 3' untranslated region (3'UTR) of the *GRIK4* gene in subjects carrying the protective haplotype. We then show, by means of a case-control association study and subsequent replication, that the deletion is significantly negatively associated with bipolar disorder; that is, it exerts a protective effect. We demonstrate in three expression systems that when both the insertion and deletion alleles are available for transcription (either actually or equivalent to the heterozygote state), *GRIK4* mRNA transcripts carrying the deletion are relatively more abundant. Differing RNA secondary structure predictions for the two allelic forms suggest a possible explanation for these findings.

## Results

**An Indel Variant Identified in the *GRIK4* 3'UTR.** Representative individuals from the original association study who were homozygous for the protective haplotype were selected and sequenced across the final *GRIK4* exon and 3'UTR. A 14-bp deletion 33 bp downstream of the stop codon was identified (Fig. 1A). Two polymorphisms at this location have been deposited in the public SNP database (dbSNP): a single A/C SNP, rs5016722, and an indel of 14 bp (-/AGGGGAGGGCGGG), rs6144536. Together, these two polymorphisms can account for the observed sequence change, but because we have not observed them individually, and the sequence in this region is repetitive in nature, we postulate that they do not exist as separate entities. Rather, we believe that a more parsimonious annotation to explain the sequence change is the existence of a single 14-bp insertion/deletion, -/CGGGGCGGGAGGGG (Fig. 1B). This has been submitted to dbSNP and granted a provisional identification number, ss79314275. The deletion co-segregates with the protective haplotype in all homozygote carriers and most of the predicted heterozygote carriers that we have tested (data not shown).

Author contributions: B.S.P., D.H.R.B., and W.J.M. designed research; B.S.P., H.M.K., R.S.H., J.K.F.B., J.M., A.M., K.A.M., and A.C. performed research; B.S.P., R.S.H., R.W., A.M., K.A.M., D.S.C., D.H.R.B., and W.J.M. contributed new reagents/analytic tools; B.S.P., H.M.K., R.S.H., D.C.S., J.K.F.B., J.M., and I.D. analyzed data; and B.S.P., R.S.H., R.W., D.J.P., D.H.R.B., and W.J.M. wrote the paper.

The authors declare no conflict of interest.

This article is a PNAS Direct Submission.

Data deposition: The data reported in this paper have been deposited in the NCBI Single Nucleotide Polymorphism database, www.ncbi.nlm.nih.gov/projects/SNP (accession no. ss79314275).

<sup>†</sup>To whom correspondence should be addressed. E-mail: ben.pickard@ed.ac.uk.

© 2008 by The National Academy of Sciences of the USA

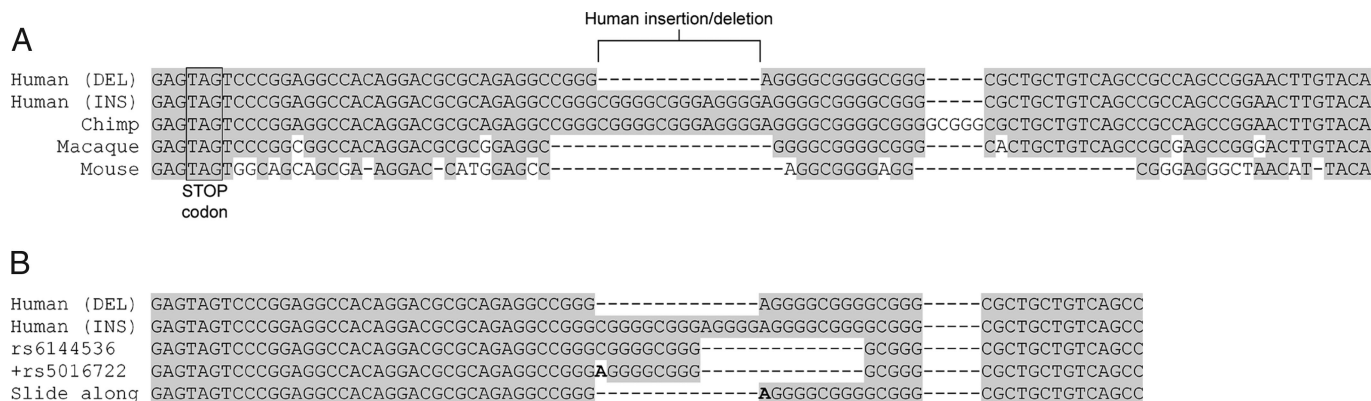


**Fig. 1.** Alignment of human (INS and DEL variants), chimp, macaque, and mouse DNA sequences surrounding the *GRIK4* 3'UTR indel. (A) The base sequence identical to human is indicated by the gray background. The 14-bp deletion in humans is labeled, as is the STOP codon at the end of the coding sequence. (B) Corrected annotation for the deletion. It can be seen that the combination of the deletion rs6144536 (third line) and SNP rs5016722 (fourth line), followed by realignment (underlined sequence in fifth line), is equivalent to the single deletion annotation, rs79314275 (top line).

**The Deletion Is Significantly Associated with Bipolar Disorder and Has a Protective Effect.** Using the polymerase chain reaction (PCR)-based genotyping assay described in *Methods*, we genotyped 356 individuals diagnosed with bipolar disorder and 286 healthy controls, a sample set largely overlapping with that of our previous SNP-based association study. Using one-tailed  $\chi^2$  analysis for both the genotype ( $P = 0.00000273$ ) and allele ( $P = 0.00000019$ ) frequencies, the deletion showed strongly significant negative association with bipolar disorder (Table 1). The deletion allele was present at a frequency of 0.24 in controls and 0.13 in individuals diagnosed with bipolar disorder, resulting in an OR of 0.4624 for the deletion allele (95% CI = 0.3445–0.6206). To confirm this finding, we carried out a replication study in an independent Scottish cohort of 274 individuals diagnosed with bipolar disorder and 376 healthy controls. Again,  $\chi^2$  analysis showed a significant negative association at the genotype ( $P = 0.0166$ ) and allele ( $P = 0.0107$ ) levels (Table 1). In this cohort, the deletion allele was present at a frequency of 0.23 in the controls and 0.17 in those with bipolar disorder, resulting in an OR of 0.6945 for the deletion allele (95% CI = 0.5245–0.9196). These data suggest that the deletion allele has

a protective effect, reducing the likelihood that a carrier will develop bipolar disorder. Although the terms “protective deletion” and “risk insertion” may be semantically equivalent, we believe the former term is more relevant because of its lower allele frequency and correlation with the original protective haplotype (no risk haplotype was discernible). We suggest that the insertion/deletion is either the actual functional variant itself or a better proxy than the original haplotype for the underlying variant.

We combined the two association data sets to have sufficient numbers to allow assessment of specific genotype effects. Comparing ORs for decreased risk of bipolar disorder associated with being either heterozygous for the deletion (OR = 0.4718; 95% CI = 0.3608–0.6169) or homozygous for the deletion (OR = 0.3258; 95% CI = 0.1836–0.5786) clearly shows that the protection afforded by the deletion is additive/dose-dependent, entirely consistent with the evidence for transcript regulation presented below.

***GRIK4* Transcripts Containing the Deletion Are Present at Relatively Higher Cellular Levels than Those with the Insertion.** Using the same PCR-based genotyping assay, we were able to quantify the relative proportions of the two *GRIK4* alleles (insertion and deletion) expressed in three experimental systems: a naturally heterozygous neuroblastoma cell line (SHSY-5Y), a human embryonic kidney HEK293 cell line transfected with *GRIK4* expression constructs, and a set of postmortem brain tissue samples from heterozygous individuals with no psychiatric illness. Although heterozygote genomic DNA, as a test of the assay's accuracy, demonstrated nearly equal allelic representation, as expected (Fig. 2), cDNA samples from the SHSY-5Y neuroblastoma cells, reflecting endogenous mRNA abundance, all showed a marked predominance of the deletion allele, indicating its increased relative prevalence (Fig. 2B). This was the case for both reverse-transcription (RT) primers used (oligo dT and p1; see *Methods*), indicating that polyadenylation extent, RT biases, and preferential 3' end mRNA degradation are unlikely explanations for this phenomenon.

But these findings did not exclude the possibility that *cis*-regulatory elements in linkage disequilibrium with the insertion or deletion alleles might be responsible for the expression bias, rather than the variant itself. To examine this hypothesis, we constructed two plasmid expression vectors (see *Methods*) driving expression of a *GFP-GRIK4* final coding exon and partial 3'UTR fusion that differed only in the presence or absence of the 3'UTR deletion variant. Equal proportions of the insertion and deletion forms of the

**Table 1. Indel genotyping results from individuals diagnosed with bipolar disorder and healthy controls in the original and replication studies**

Genotype/Allele	Control	Bipolar	Total	<i>P</i>
<b>Original study</b>				
DEL/DEL	20	11	31	
DEL/INS	95	67	162	
INS/INS	171	278	449	
Total	286	356	642	0.00000273
DEL	135	89	224	
INS	437	623	1,060	
Total	572	712	1,284	0.00000019
<b>Replication study</b>				
DEL/DEL	25	6	31	
DEL/INS	121	81	202	
INS/INS	230	187	417	
Total	376	274	650	0.0166
DEL	171	93	264	
INS	581	455	1,036	
Total	752	548	1,300	0.0107

$\chi^2$  test-derived *P* values are shown for the individual genotype and allele frequency tables.

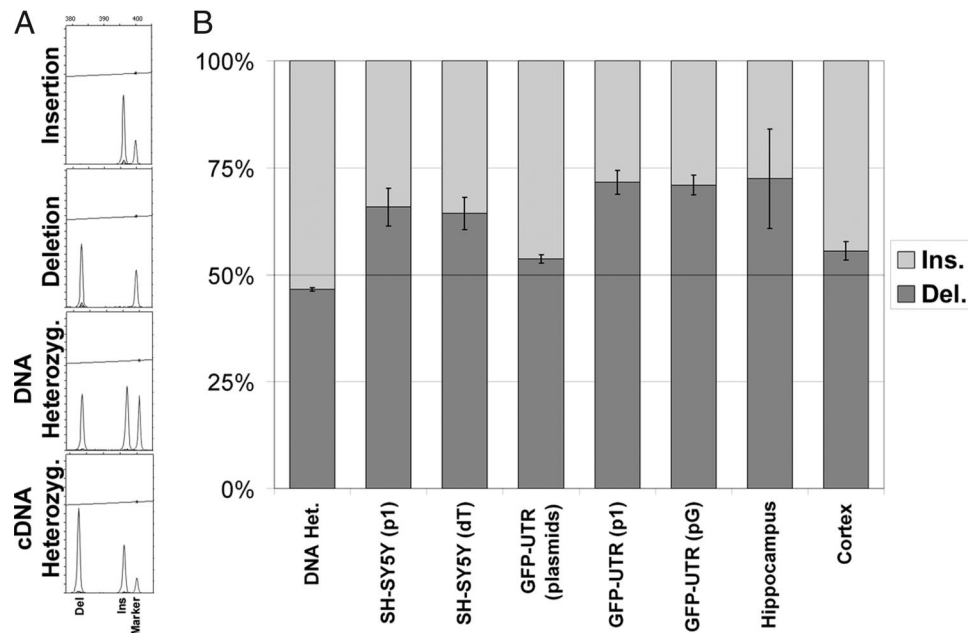


**Fig. 2.** Relative expression levels of the deletion and insertion *GRIK4* alleles as determined by fluorescent-labeled PCR. (A) Representative examples from the PCR assay. The FAM-labeled insertion and deletion PCR products are shown next to a 400-bp size marker. (B) Proportions of the insertion and deletion forms in SHSY-5Y genomic DNA ( $n = 3$ ), cDNA samples from SHSY-5Y (two separate RT primers;  $n = 6$ ), pretransfection insertion/deletion expression plasmid mix (assay replicated three times), cDNA from HEK293 cells transfected with the insertion/deletion expression plasmid mix (two separate RT primers;  $n = 5$ ), and cDNA from heterozygote control human hippocampus (three samples) and cortex (five samples). Error bars indicate the standard error of the mean.

plasmids were mixed and then transiently transfected into HEK293 cells. Both the initial plasmid mix (to set the experimental baseline for equal allelic representation) and the transfected cell line cDNA (two separate RT primers, one of which, g1', was directed at vector-specific 3'UTR sequences to differentiate exogenous and endogenous transcripts) were assayed for relative allelic abundance using the PCR assay. Again, the input plasmid DNA showed almost equivalent allelic representation, whereas a clear overrepresentation of the deletion-carrying mRNA was observed regardless of RT primer (Fig. 2B). This transfection approach, through isolation of the indel effect from *cis* effects, suggests that the variant alone is responsible for the observed expression bias.

Finally, we wished to examine the effect of the deletion in humans. Using the genotyping assay, we identified diagnostically unaffected heterozygous individuals from a brain tissue repository. RNA from hippocampus and cerebral cortical brain regions was extracted, reverse-transcribed, and assayed as above. Despite the relatively small sample size and potential variability in tissue quality and pathological state, we observed a similar bias toward overrepresentation of the deletion-carrying transcript, particularly in the hippocampus (Fig. 2B).

We suggest that this expression assay is likely to prove more accurate and less prone to RNA quality issues compared with other quantitative PCR approaches that require expression normalization using separately assayed reference genes (e.g., *GAPDH*).

**RNA Secondary Structure and the Indel.** Comparison of the INS- and DEL-containing secondary structures revealed two distinct populations of secondary structures. The INS-containing sequences for human and chimp are highly conserved and thus form secondary structures with a high degree of consensus (Fig. 3A, D, and G). The consensus structure does not necessarily represent actual structures for the contributing structures; rather, the structure that is consistent among all structures. The chimp sequence has an extra insert (GCGGG) (Fig. 1A), resulting in an enlarged bulge in the consensus secondary structure prediction

(Fig. 3D). This extra insert appears to have a stabilizing effect, because fewer possible stable structures are predicted in the chimp sequence ( $n = 1$ ) compared with the human sequence ( $n = 3$ ). The DEL sequences ( $n = 16$ ), with the mouse sequence included, do not form any consistent structure, because only four base pairs are present in all structures (Fig. 3B, E, and H); however, removal of the mouse sequences reveals a greater degree of consensus in the structures ( $n = 14$ ) (Fig. 3C, F, and I). This consensus structure is clearly different from that of the INS sequences, indicating a possible functional difference between the structures.

## Discussion

This paper presents further evidence to support the involvement of *GRIK4* in the etiology of psychiatric illness and builds on our original identification of *GRIK4* gene disruption by a rare cytogenetic rearrangement and its involvement in altered risk of schizophrenia and bipolar disorder in the wider population. We observed a highly significant association between a newly identified 3'UTR deletion variant in the gene and protection against bipolar disorder. This finding was replicated in an independent Scottish sample of comparable size. Although this variant may be a tightly linked proxy for the actual pathological mutation, its location within the transcript and isolated activity in transfection experiments formally suggest that it is the functional change underlying the original protective haplotype association.

It must be noted that the recent Wellcome Trust Case Control Consortium genome-wide association study of bipolar disorder failed to highlight *GRIK4* as a candidate (19). But examination of the coverage of the GeneChip 500K Mapping Array Set (Affymetrix) used in that study shows that only one (rs2282586) of the two SNPs that give rise to the strongest original associated protective haplotype (and only one of the five SNPs that compose the extended haplotype) was present on the chip. In isolation, rs2282586 showed only a moderately significant association ( $P = 0.02$ ) in our original study and thus may not have met the stringent requirements for significance in a genome-



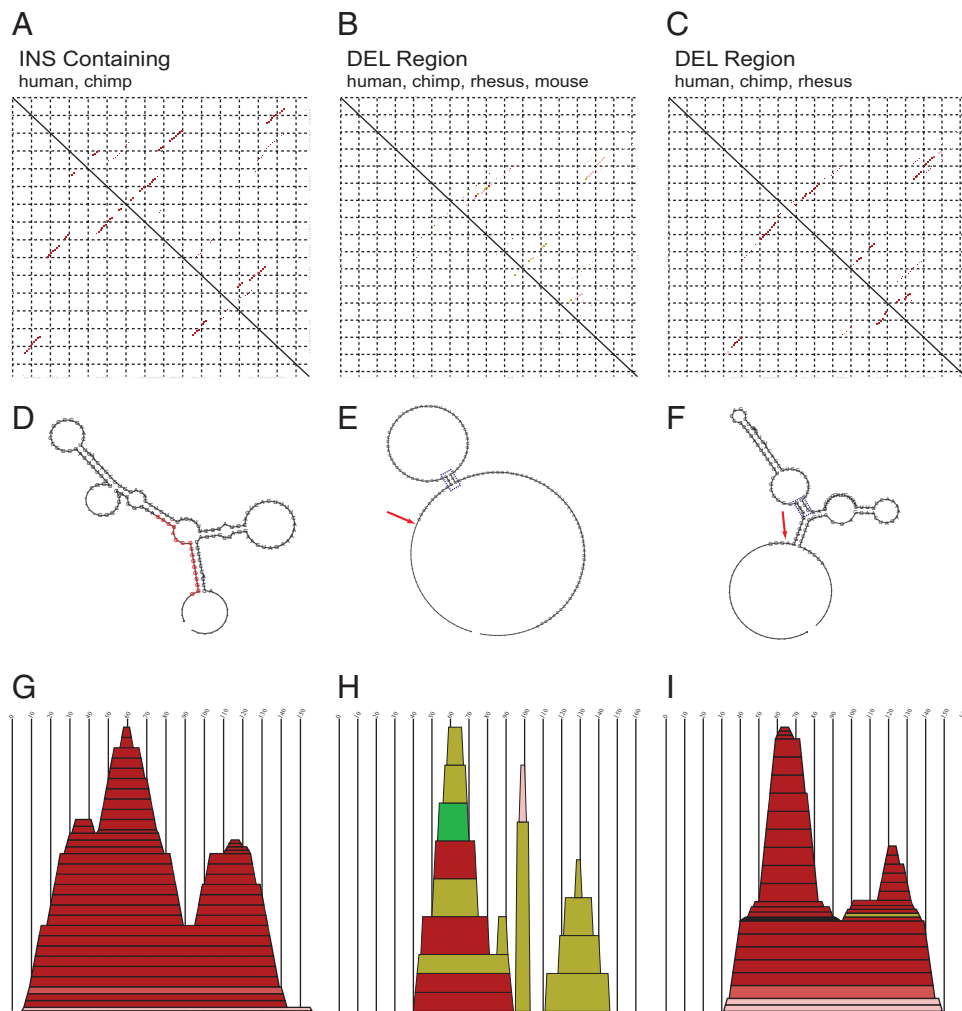


**Fig. 3.** RNA secondary structure predictions of the INS- and DEL-containing *GRIK4* sequences show clear differences. Dot plots for the RNA secondary structures of the sequences shown in part in Fig. 1A. The dot plots show predicted base pairings for the sequences. The bottom-left diagonal of each dot plot shows only the most conserved base pairings. The upper-right diagonal shows predicted base pairings inconsistent with all sequences in the alignment. The saturation of the dots is correlated inversely with the number of inconsistencies (saturated for no inconsistencies). The colors of the dots correspond to the frequency of types of base pairings present, to highlight compensatory mutations (red, 1; ochre, 2; green, 3; turquoise, 4; blue, 5; violet, 6). The axes of the dot plots correspond to the consensus secondary structure predictions. (A) Dot plot for the INS-containing sequences from human and chimp. (B) Dot plot for the DEL-containing sequences (human, chimp, rhesus, mouse). (C) As in (B), but with the more divergent mouse sequences removed. Two additional visualizations of these data are shown directly beneath each dot plot. (D–F) Consensus secondary sequence and structure predictions, corresponding to the lower-left diagonal of the dot plots above. The INS sequence is colored red, and the position of the DEL is highlighted with a red arrow. Conserved base pairings between (E) and (F) are shown in the blue-dashed boxes. (G–I) Mountain plots for the consensus structure predictions, corresponding to the upper right diagonal of the dot plots above.

wide study. Therefore, further replication of this strong association in both European and non-European (but probably not Asian) populations remains an important future confirmation. It will be particularly important to ensure the testing of similarly structured cohorts, predominantly sporadic cases, because we consider this a nonfamilial common variant.

Allelic expression analyses in the SHSY-5Y neuroblastoma cell line, transiently transfected cells, and postmortem tissue heterozygote for the indel repeatedly demonstrated a greater proportion of the deletion-bearing mRNA. This is not likely the result of increased transcription rate but rather suggests that *GRIK4* mRNA stability may be the 3'UTR property altered by the indel. These data attractively link the genetically protective nature of the deletion allele with increased *GRIK4* expression in the context of the hypothesis that glutamate neurotransmission levels are an important risk factor in mental illness. From the allelic ratio experiment, we calculate that the absolute expression level increase between *GRIK4* insertion homozygotes and dele-

tion heterozygotes is  $\approx 40\%$ . Studies are currently underway to examine the effects of indel status on *GRIK4* protein levels and histological and subcellular localization. Such studies may provide an explanation for the absence of genotype effect on *GRIK4* expression in the cortex compared with the hippocampus (Fig. 2B).

The increased frequency of indels in 3'UTRs compared with other gene regions has been noted in a transcriptome annotation publication (20) and the ENCODE project (21, 22) and may reflect higher GC content and/or low-complexity sequences (both of which were evident in the *GRIK4* 3'UTR). One interpretation of this finding is that 3'UTRs may be permissive of indels, because of an overall reduction in functional constraints on the sequence. Alternatively, it may indicate a positively selected role for indels in the functional modification of the transcript, perhaps because indels, unlike SNPs, can perturb local RNA secondary structures. Supporting this latter conjecture, one study (23) found that 3'UTR deletions of as little as 5

bp are likely to result in mRNA secondary structure changes and, by inference, functional alterations in important processes regulated by 3'UTRs, such as polyadenylation, mRNA stability, subcellular transport, and translational efficiency. Numerous pathological 3'UTR mutations have been identified and summarized in the literature (24, 25). Here the size of the *GRIK4* indel and its location within a region of possible secondary structure are consistent with a role in *GRIK4* mRNA regulation. The indel region of the 3'UTR does not contain AU-rich elements, which have been implicated in posttranscription regulation of, for example, *CDK5RI* mRNA through increased mRNA degradation (26, 27); however, the region is AG-rich, a feature linked to increased likelihood of single-stranded RNA conformation. Such single-stranded stretches can facilitate interactions with other macromolecules, as in the case of hnRNA binding to human *CYP2A6* mRNA (28). Our consensus structure for the INS sequence shows that several regions exist as single strands and thus are potential targets for specific protein factor or miRNA binding. Indeed, the 14-nucleotide insertion itself forms a single-stranded region of 3 nucleotides, composing part of an internal loop in the structure. Subsequent to the binding of a factor (miRNA or protein) to a short, single-stranded stretch of RNA, a conformational change may occur to induce fitting of the RNA-plus factor (29). Biochemistry pull-down experiments are needed to explore the mechanism by which the indel exerts its effects, perhaps through the identification of putative partners differentially binding the INS and DEL sequences.

Another link between this receptor and mental illness has been described recently. SNPs in the *GRIK4* and *5HTR2A* genes have been linked to the responsiveness of depressed patients to citalopram, a serotonin reuptake inhibitor antidepressant (30). Whether these variants are related to the schizophrenia or bipolar variants that we have detailed or represent novel functional variation within the gene remains to be clarified. The *GRIK4* findings presented here raise the possibility that pharmacologically mediated increases in kainate receptor activity, mirroring the protective deletion's effect on expression, might present a therapeutic opportunity for bipolar disorder and other psychiatric illnesses.

## Methods

**Genotyping and Relative Expression Assay.** The following PCR protocol was used for both the genotyping and expression components of this study. PCR was performed on genomic DNA (genotyping), plasmid DNA mix (baseline for transient transfection experiments), or treated DNaseI (to remove genomic/plasmid DNA carryover) total RNA reverse-transcribed into cDNA (relative expression analysis). The following RT primers were used: oligo dT: dT; TCT-GTAAGAAGACTAGACGGA: p1'; GCAAACAACAGATGGCT: pG. dT primes all polyadenylated transcripts, p1 primes only *GRIK4* transcripts, and pG primes only transcripts expressed from the *GFP-GRIK4* fusion expression construct described below. PCR amplification was performed on the DNA or cDNA using primers: FAM-labeled GTGGGAGAAAACCAACA and GGGGAAAT-TCAACTGATGAT. An MJ Research PTC-225 DNA Engine Tetrad cyclor was used to perform the cycling under the following conditions: 94°C for 2 min, [94°C for 45 s, 57°C for 1 min, 72°C for 45 s] for seven cycles, [94°C for 45 s, 56°C for 1 min, 72°C for 45 s] for seven cycles, [94°C for 45 s, 55°C for 1 min, 72°C for 45 s] for 26 cycles, and 72°C for 15 min. Taq polymerase (Sigma), reaction buffer 1 from the Expand LongRange PCR kit (Roche), and PCR Enhance (Invitrogen) were found to provide optimal amplification.

Products were diluted 400-fold and then resolved on an ABI 3730 analyzer (Applied Biosystems), with peak volumes analyzed using Applied Biosystems Peak Scanner v1.0 freeware. For the genotyping, no significant deviation from the Hardy-Weinberg equilibrium was detected for this assay in healthy controls of the original or replication cohorts ( $P = 0.182$  and  $0.103$ , respectively).

**Case-Control Association Study.** The indel variant was genotyped in 356 individuals with bipolar disorder and 286 healthy controls from Scotland. These DNA samples largely overlap with those used in our previous SNP-based case-control association study, and information concerning their diagnosis

and provenance is provided in that paper (8). Informed consent was obtained from all individuals donating blood for DNA extraction, and the study design was approved by the MultiCentre Research Ethics Committee for Scotland. The replication sample set comprised 376 healthy controls and 111 (of a total of 274) cases diagnosed with bipolar disorder from northeastern Scotland, together with 163 cases from southeastern Scotland. The diagnostic workup for these samples from northeastern Scotland followed the same procedures as for the first set, with clinical diagnoses made by D.St.C. Again, full informed consent from all individuals was obtained, and the study design was approved.

**Transient Transfection Experiments.** Expression plasmids containing either the deletion or insertion alleles were constructed using Invitrogen Gateway system pDONR and pcdna-DEST53 vectors by amplifying genomic DNA from homozygous insertion or deletion individuals using the primers GGGGA-CAAGTTTGACAAAAAGCAGGCTGTGTGTCAGGACAGTATCCACCC and GGG-GACCACTTTGTACAAGAAAGCTGGGTTAATCCATGATAGTCTTGGGG, which also contain homologous recombination ends for the BP and LR enzymatic reactions (italicized). The cloned *GRIK4* sequences compose the majority of the final coding exon sequence and  $\approx 1$  kb of 3'UTR. The open reading frame between the pDEST53 vector green fluorescent protein (*GFP*) and *GRIK4* sequences was maintained such that a fusion mRNA and protein resulted. Plasmid inserts were fully sequenced to ensure correct incorporation of *GRIK4* insertion or deletion sequences. Equal quantities (as determined by spectroscopic DNA quantification) of the two expression constructs were combined and transfected into HEK293 cells using Lipofectamine 2000 (Invitrogen) according to manufacturer's directions. After 24 h of transfection in serum-free conditions, the growth medium was replaced by 10% fetal bovine serum-supplemented Dulbecco's modified Eagle medium. Cells were cultured for another 24 h and then harvested using trypsin/versene in preparation for total RNA extraction using a RNeasy Mini Kit and on-column DNaseI digestion (Qiagen).

**Postmortem Brain Sample RNA Extraction.** Frozen samples from histologically characterized normal brain tissues that were authorized for ethically approved scientific investigation were obtained from the Medical Research Council Sudden Death Brain & Tissue Bank, Edinburgh (31) and genotyped for indel status. Heterozygotes were selected and tissue samples dissected from the superior frontal gyrus (cortex;  $n = 5$ ) and the hippocampus ( $n = 3$ ). Total RNA was extracted using the lipid-rich tissue RNeasy Kit (Qiagen), again using on-column DNaseI digestion to ensure no genomic DNA carry-over. RNA integrity number (RIN) values, the proprietary total RNA quality scores generated using the Agilent BioAnalyzer platform, were calculated for the brain RNA samples and showed a considerable variation, from 2.1 to 6.8 (maximum possible value, 10), demonstrating that some samples evidenced partial degradation. Despite this, however, no clear correlation was observed between RIN value and relative expression level (data not shown), indicating that a relative allelic expression level assay such as this is generally resistant to biases resulting from RNA sample quality issues.

**RNA Secondary Structure Prediction.** Because most RNA readily forms secondary structures, it was necessary to determine whether the structures were thermodynamically stable and/or conserved across species to indicate whether they were likely to be functionally important. *GRIK4* sequences for human DEL, human INS, chimp, rhesus, and mouse were tested for locally stable structures using RNALfold (32), which folds RNA in sliding windows incrementing one base at a time.

Recent studies have shown that in addition to sequence recognition, the local secondary structure of the RNA target sites for miRNA and siRNA are of key importance to binding. For example Zhao *et al.* (33) showed that miRNAs preferentially bind 3'UTR regions accessible as less complex structures (not tight stem loops), but not in unstructured regions (entirely single-stranded). Overhoff *et al.* (34) found that the binding of siRNAs to their target RNA also is affected by the secondary structure of the target RNA. Long *et al.* (35) proposed a two-step binding of miRNAs to their targets where a short region of RNA sequence with a key secondary structure is bound, before a second step of secondary structure relaxation and binding elongation. Heale *et al.* (36) also showed that the locally stable substructures of target RNAs are important for the interaction with siRNA in mammalian cells.

The minimum free energy (MFE) stable structures were filtered for the indel region of the sequences and separated into two groups, INS-containing and DEL-containing. In an additional step, suboptimal secondary structures for each stable structure were generated using UNAFold (37) to determine the variance of possible secondary structures for each of the stable structures. Visual inspection of the structures confirmed the existence of two distinct populations of structures, one for INS-containing sequences and one for

DEL-containing sequences. The original stable MFE structures from RNALfold for the INS- and DEL-containing structures were used to generate multiple sequence alignments using MUSCLE (38). Manual adjustment of the alignments was required for the DEL-containing sequences. Because the mouse sequence does not align well in this region, alignments were created with and without the mouse sequences. Consensus structure prediction was performed using Alidot (39, 40), which exploits sequence variability in the input alignments to determine a consensus within the structures. The alignments from the INS and DEL (with and without mouse) sequences with the stable structures (MFE) were used as input for Alidot. Base pairings for each structure in the alignment are assessed for their likelihood of being maintained across the whole alignment; for instance, compensatory mutations to maintain base pairs are considered a good indication that a base pair is required for RNA

function. The output is presented in the form of dot plots. In addition, mountain plots, consensus sequences, and structures were generated, all using the Perl tools from the RNAVienna package (41).

**ACKNOWLEDGMENTS.** B.S.P. is the recipient of a Royal College of Physicians Edinburgh Sim Research Fellowship, and H.M.K. is funded by a College of Medicine and Veterinary Medicine Scholarship. R.H. and I.D. are funded by a Wellcome Trust Senior Research Fellowship (067413). Additional funding was provided by the Wellcome Trust and the Chief Scientist Office. All DNA samples were archived and handled by staff at the Wellcome Trust Clinical Research Facility at Western General Hospital, Edinburgh. Postmortem tissue samples authorized for ethically approved scientific research were kindly provided by the MRC Sudden Death Brain & Tissue Bank, University of Edinburgh.

- Belsham B (2001) Glutamate and its role in psychiatric illness. *Hum Psychopharmacol* 16:139–146.
- Farber NB (2003) The NMDA receptor hypofunction model of psychosis. *Ann N Y Acad Sci* 1003:119–130.
- Harrison PJ, Law AJ, Eastwood SL (2003) Glutamate receptors and transporters in the hippocampus in schizophrenia. *Ann N Y Acad Sci* 1003:94–101.
- McCullumsmith RE, Clinton SM, Meador-Woodruff JH (2004) Schizophrenia as a disorder of neuroplasticity. *Int Rev Neurobiol* 59:19–45.
- Moghaddam B (2003) Bringing order to the glutamate chaos in schizophrenia. *Neuron* 40:881–884.
- Morris BJ, Cochran SM, Pratt JA (2005) PCP: from pharmacology to modelling schizophrenia. *Curr Opin Pharmacol* 5:101–106.
- Tsai G, Coyle JT (2002) Glutamatergic mechanisms in schizophrenia. *Annu Rev Pharmacol Toxicol* 42:165–179.
- Pickard BS, et al. (2006) Cytogenetic and genetic evidence supports a role for the kainate-type glutamate receptor gene, GRIK4, in schizophrenia and bipolar disorder. *Mol Psychiatry* 11:847–857.
- Bortolotto ZA, Nistico R, More JC, Jane DE, Collingridge GL (2005) Kainate receptors and mossy fiber LTP. *Neurotoxicology* 26:769–777.
- Darstein M, Petralia RS, Swanson GT, Wenthold RJ, Heinemann SF (2003) Distribution of kainate receptor subunits at hippocampal mossy fiber synapses. *J Neurosci* 23:8013–8019.
- Kamboj RK, et al. (1994) Molecular cloning, expression, and pharmacological characterization of humEAA1, a human kainate receptor subunit. *J Neurochem* 62:1–9.
- Kask K, et al. (2000) Developmental profile of kainate receptor subunit KA1 revealed by Cre expression in YAC transgenic mice. *Brain Res* 876:55–61.
- Lerma J (2006) Kainate receptor physiology. *Curr Opin Pharmacol* 6:89–97.
- Pinheiro P, Mulle C (2006) Kainate receptors. *Cell Tissue Res* 326:457–482.
- Fogarty DJ, Perez-Cerda F, Matute C (2000) KA1-like kainate receptor subunit immunoreactivity in neurons and glia using a novel anti-peptide antibody. *Brain Res Mol Brain Res* 81:164–176.
- Kerwin R, Patel S, Meldrum B (1990) Quantitative autoradiographic analysis of glutamate binding sites in the hippocampal formation in normal and schizophrenic brain postmortem. *Neuroscience* 39:25–32.
- Meador-Woodruff JH, Davis KL, Haroutunian V (2001) Abnormal kainate receptor expression in prefrontal cortex in schizophrenia. *Neuropsychopharmacology* 24:545–552.
- Sokolov BP (1998) Expression of NMDAR1, GluR1, GluR7, and KA1 glutamate receptor mRNAs is decreased in frontal cortex of “neuroleptic-free” schizophrenics: evidence on reversible up-regulation by typical neuroleptics. *J Neurochem* 71:2454–2464.
- Anonymous (2007) Genome-wide association study of 14,000 cases of seven common diseases and 3,000 shared controls. *Nature* 447:661–678.
- Imanishi T, et al. (2004) Integrative annotation of 21,037 human genes validated by full-length cDNA clones. *PLoS Biol* 2:e162.
- Birney E, et al. (2007) Identification and analysis of functional elements in 1% of the human genome by the ENCODE pilot project. *Nature* 447:799–816.
- Clark TG, et al. (2007) Functional constraint and small insertions and deletions in the ENCODE regions of the human genome. *Genome Biol* 8:R180.
- Chen JM, Ferec C, Cooper DN (2006) A systematic analysis of disease-associated variants in the 3' regulatory regions of human protein-coding genes, I: general principles and overview. *Hum Genet* 120:1–21.
- Chen JM, Ferec C, Cooper DN (2006) A systematic analysis of disease-associated variants in the 3' regulatory regions of human protein-coding genes, II: the importance of mRNA secondary structure in assessing the functionality of 3' UTR variants. *Hum Genet* 120:301–333.
- Conne B, Stutz A, Vassalli JD (2000) The 3' untranslated region of messenger RNA: a molecular “hotspot” for pathology? *Nat Med* 6:637–641.
- Bevilacqua A, Ceriani MC, Capaccioli S, Nicolini A (2003) Post-transcriptional regulation of gene expression by degradation of messenger RNAs. *J Cell Physiol* 195:356–372.
- Moncini S, et al. (2007) The 3' untranslated region of human cyclin-dependent kinase 5 regulatory subunit 1 contains regulatory elements affecting transcript stability. *BMC Mol Biol* 8:111.
- Christian K, Lang M, Maurel P, Raffalli-Mathieu F (2004) Interaction of heterogeneous nuclear ribonucleoprotein A1 with cytochrome P450 2A6 mRNA: implications for post-transcriptional regulation of the CYP2A6 gene. *Mol Pharmacol* 65:1405–1414.
- Shajani Z, Deka P, Varani G (2006) Decoding RNA motional codes. *Trends Biochem Sci* 31:421–424.
- Paddock S, et al. (2007) Association of GRIK4 with outcome of antidepressant treatment in the STAR\*D cohort. *Am J Psychiatry* 164:1181–1188.
- Millar T, et al. (2007) Tissue and organ donation for research in forensic pathology: the MRC Sudden Death Brain and Tissue Bank. *J Pathol* 213:369–375.
- Hofacker IL, Priwitzer B, Stadler PF (2004) Prediction of locally stable RNA secondary structures for genome-wide surveys. *Bioinformatics* 20:186–190.
- Zhao Y, Samal E, Srivastava D (2005) Serum response factor regulates a muscle-specific microRNA that targets Hand2 during cardiogenesis. *Nature* 436:214–220.
- Overhoff M, et al. (2005) Local RNA target structure influences siRNA efficacy: a systematic global analysis. *J Mol Biol* 348:871–881.
- Long D, et al. (2007) Potent effect of target structure on microRNA function. *Nat Struct Mol Biol* 14:287–294.
- Heale BS, Soifer HS, Bowers C, Rossi JJ (2005) siRNA target site secondary structure predictions using local stable substructures. *Nucleic Acids Res* 33:e30.
- Zuker M (2000) Calculating nucleic acid secondary structure. *Curr Opin Struct Biol* 10:303–310.
- Edgar RC (2004) MUSCLE: a multiple sequence alignment method with reduced time and space complexity. *BMC Bioinformatics* 5:113.
- Hofacker IL, et al. (1998) Automatic detection of conserved RNA structure elements in complete RNA virus genomes. *Nucleic Acids Res* 26:3825–3836.
- Hofacker IL, Stadler PF (1999) Automatic detection of conserved base pairing patterns in RNA virus genomes. *Comput Chem* 23:401–414.
- Hofacker IL (2003) Vienna RNA secondary structure server. *Nucleic Acids Res* 31:3429–3431.